JMEPEG (1999) 8:211-218

Mechanical Response and Failure of Bolted Connection Elements in Aluminum Alloy 5083

C.C. Menzemer, L. Fei, and T.S. Srivatsan

(Submitted 27 April 1998; in revised form 23 September 1998)

In a spectrum of structures made from pure aluminum and aluminum-base alloys, plates are used frequently as the choice candidate for connecting elements. Design of safe, efficient, and reliable connections necessitates that adequate consideration be given to failure of the fastener element, distress of material in the immediate vicinity of the fastener(s), tensile failure of the net section, and even tear out of the fastener group(s). The mechanical response and failure characteristics of aluminum connecting elements are presented and discussed in this paper. An experimental and analytical program was conducted to rationalize failure of connecting elements made from an aluminum-magnesium alloy. Gusset plates representing different bolt patterns were mechanically deformed. Models to estimate the capacity of the joints were examined and compared with experimentally determined results.

Keywords aluminum alloy, connection element, failure, stress-analysis, tensile deformation

1. Introduction

A wide spectrum of structures in the industries of construction and transportation (both air and ground) are built from either pure aluminum or aluminum-base alloys. Plates have been used frequently as connecting links for such structures. A few noteworthy examples include bracing systems and structural elements in railcars, framing members in bulk transport vehicles and containers, mounts for dump bodies, and framing nodes for roof trusses. Mechanical fasteners also can be utilized in situations when there exists a conjoint need for ease of application, familiarity with fabrication processes, and concerns with severe dynamic loading. A technically safe and sound design necessitates that adequate consideration be given to failure of the fasteners, failure of the connection plate(s), and the role and durability of the attaching members. Current design specifications spanning the branches of mechanical and civil (structural) engineering either make use of models developed for structural steels or leave estimation of capacity to the discretion of the design or practicing engineer (Ref 1, 2).

Mechanical fasteners are good for the transfer of load over relatively small areas. Consequently, design issues encountered with intrinsic details are normally associated with the transfer of concentrated forces (Ref 3). Failure of a single rivet or bolt in a lap joint can take place as a result of the independent or conjoint and mutually interactive influences of (a) shear failure of the fastener, (b) progressive bearing distress of material adjacent to the fastener, (c) splitting of the sheet or plate near the fastener hole in the direction of the applied load, and (d) tensile overload failure of the net section (Ref 4). A balance between the different failure modes provides an attractive and viable means for establishing the minimum edge distances and fastener spacing.

Plates of relatively thin cross-sectional area and even extruded shapes fastened using one or more components tend to frequently fail by the tearing out of a piece of material along the periphery of the bolt or rivet group. The block shear failure mode for a gusset plate and a single angle member when subjected to the influence of a far-field tensile load is shown in Fig. 1. In each case, failure occurs by the removal of material around the immediate periphery of the bolt group. In the case of the single angle, load is essentially transferred by tension along a horizontal plane defined by the edge of the member and the first bolt or rivet, while shear stresses develop along the line of fasteners. A similar situation exists for the gusset or connecting element. A combination of tensile and shear stresses develop along an area defined by the periphery of the fastener group. Another practical example that demands consideration of block failure are simple shear connections in beams having coped flanges (Ref 5).

There is a paucity of research work on evaluating and understanding block failures of mechanical connections made from pure aluminum and aluminum-base alloys. In 1992 Sharp documented findings on the behavior of angles fastened by a single leg (Ref 4). Extruded angles of aluminum alloy 6061-T6 were connected at the ends by using a varying number of bolts made from aluminum alloy 2024-T4. Subsequently, those angles were mechanically deformed to failure. As expected, the failure mode changed as a function of the number of fasteners. Angles connected by a single bolt failed predominantly by shear and bearing of the angle. However, those angles connected by two bolts failed by block shear, while angles with connections having three or more bolts exhibited failure at the net section as a result of tensile overload. Marsh developed a model to estimate the capacity of bolt groups based upon data from double lap joints fabricated from sheet stock of aluminum alloy 6063-T6 (Ref 6). Edge distance, gage spacing and pitch spacing were treated as variables. Multiple tests were conducted on specimens having different geometry. The model proposed to estimate joint capacity was a function of

C.C. Menzemer and L. Fei, Department of Civil Engineering, University of Akron, Akron, OH 44325, USA; **T.S. Srivatsan,** Department of Mechanical Engineering, University of Akron, Akron, OH 44325-3903, USA.

the following variables: (a) distance around the bolt group perimeter, (b) thickness of the sheet stock, and (c) ultimate tensile strength (σ_{uts}) of the base material.

Analytical predictions of strength generally corresponded to the experimentally determined values within several percentage points, excluding those predictions and values for joints that failed by shearing along a single fastener line. It is the objective of this paper to discuss the mechanical response and failure of connection elements made from an aluminum alloy (Aluminum Association designation 5083).

2. Material and Experimental Techniques

The commercial non-heat-treatable aluminum-magnesium alloy 5083 was chosen for this study. The nominal chemical composition of the alloy (in wt%) is given in Table 1. The amount of magnesium (4.0 wt%) soluble at the annealing temperature of the alloy is higher than the amount of magnesium retained in solid solution at room temperature (Ref 7). Due to the limited solubility of the Mg_2Si in pure aluminum, Mg_2Si is present in the microstructure as a major constituent phase (Ref 7). The presence of manganese results in the precipitation of the dispersoids during ingot preheat and high-temperature homogenization treatments. Preheating of the 5083 ingot aids in eliminating the magnesium coring of the dendrite, which occurs during solidification. Copper is present primarily for the purpose of corrosion protection. Magnesium has low solubility in aluminum and precipitates as a ternary compound during solidification and preheating (Ref 7, 8). In wrought sheet stock, copper is present as the compound $A1_{12}Mg_2Cu$ (denoted as the E phase) as a result of precipitation during preheat. The magnesium in solution imparts limited solid-solution strengthening effect to the aluminum alloy matrix. Also, magnesium is important as a strengthening element through its influence on work hardening. The conjoint influence of magnesium in solution and cold deformation is responsible for the acceptable strength of this aluminum alloy. Additional strengthening is provided by the manganese in solution that aids in decreasing the recrystallized grain size. The 5083 material was received in the strain hardened temper (H321).

Table 1 Nominal chemical composition of aluminum alloy 5083 (Ref 15)

Chemical	Composition, wt%
Mg	4.0
Cu	0.10
Mn	0.40
Fe	0.40
Al	94.20

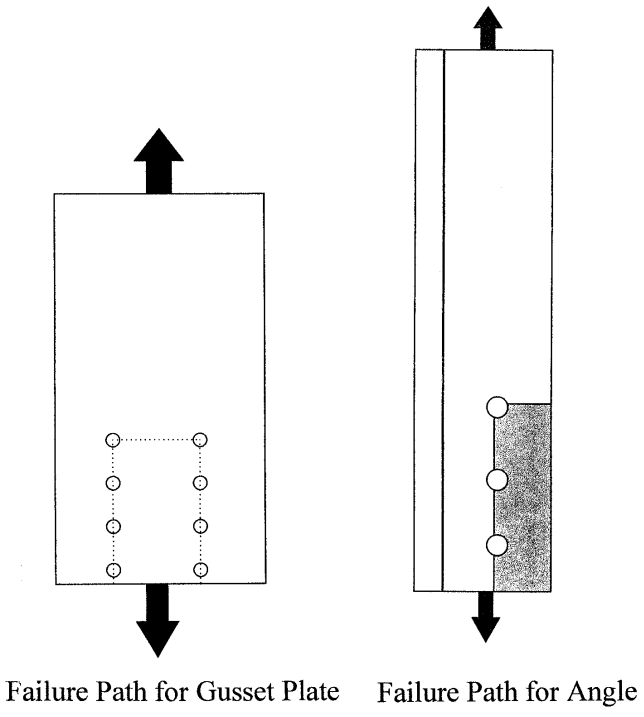

Fig. 1 Block shear failure mode for a connection plate and angle

Three gusset plates were fabricated and mechanically deformed in tension (Ref 9). As a number of variables control the behavior of mechanically fastened joints in aluminum alloys, only the most influential were considered in this study. These included specimen geometry, that is, variation in joint length, and fastener gage spacing. The other variables that were not examined include edge distance, pitch, and specimen thickness. Three different specimen types were chosen for evaluation (Fig. 2). Specimen SH1 provided for the combination of shortest gage (50 mm) and overall joint length. In this instance, gage is defined as the distance between the lines or rows of fasteners. The test specimen SH2 maintained the same overall joint length as SH1 but had twice the gage spacing (Fig. 2b). The sample SH3 utilized a combination of narrow gage (50 mm) and twice the overall joint length (Fig. 2c).

Three specimens were precision fabricated from 6.25 mm thicknesses of aluminum alloy 5083-H321 and were oriented transverse to the direction of mechanical working. The samples were mechanically deformed using fasteners that were high-strength steel bolts of size 16 mm. The gusset plate samples were prepared from mill quality plates. Samples were sheared from blanks. Subsequently, a master template was constructed by transferring all hole locations from the steel test fixture to a blank sample. The template was utilized for the hole layout of each connection plate. Holes on the test samples were made 1.5 mm oversize to reflect actual fabrication practice and also to account for possible errors in the layout process.

The mechanical tests were conducted on a 300 kip Warner-Swasey (Giddings and Lewis, Inc., Fond du Lac, WI) universal testing machine (UTM). Displacement was measured at two points on the lower crosshead using a pair of linear variable displacement transducers (LVDT). The strains were measured by mounting strain gages around the periphery of the connection plate. Strain gages were placed on the specimen so as to lie on the outer periphery of the steel fixture. The strain and displacement data were concurrently recorded on a Micro-Measurement System 5000 (Measurements Group, Inc., Raleigh, NC) acquisition system (Ref 10). At periodic intervals, the load was read from a dynamometer and subsequently entered onto spreadsheets to produce variations of load versus displacement, and load versus strain.

Failure surfaces were prepared from the deformed and failed sample (SH2) and examined in the scanning electron microscope (SEM) at low magnifications to establish the macroscopic fracture mode and at higher magnifications to establish the intrinsic micromechanisms governing fracture. Microscopy observations would concurrently facilitate establishing a correlation between the governing failure mechanisms with the failure model.

3. Results and Discussion

3.1 Mechanical Response

The load versus displacement response for the gusset plate is as shown in Fig. 3. The bolts were brought to a snug fit condition prior to the initiation of mechanical testing. No effort was made to roughen the surfaces of the aluminum alloy specimens. Consequently, load was expected to be transferred predominantly by bearing. However, at the limit, the transfer of load by bearing would be expected because most friction-type connections are proportioned at the service level load. The load-displacement record revealed an absence of a horizontal plateau during elastic loading, considered essential for sudden slip into bearing. The load-displacement curves for the deformed samples revealed a gradual increase in slope during the early stages of testing. Such behavior is rationalized as being indicative of the removal of slack from the load train and a gradual slip into bearing. However, such behavior was not evident when the specimen was preloaded prior to the initiation of mechanical testing, and the load versus displacement record was essentially linear in the elastic region.

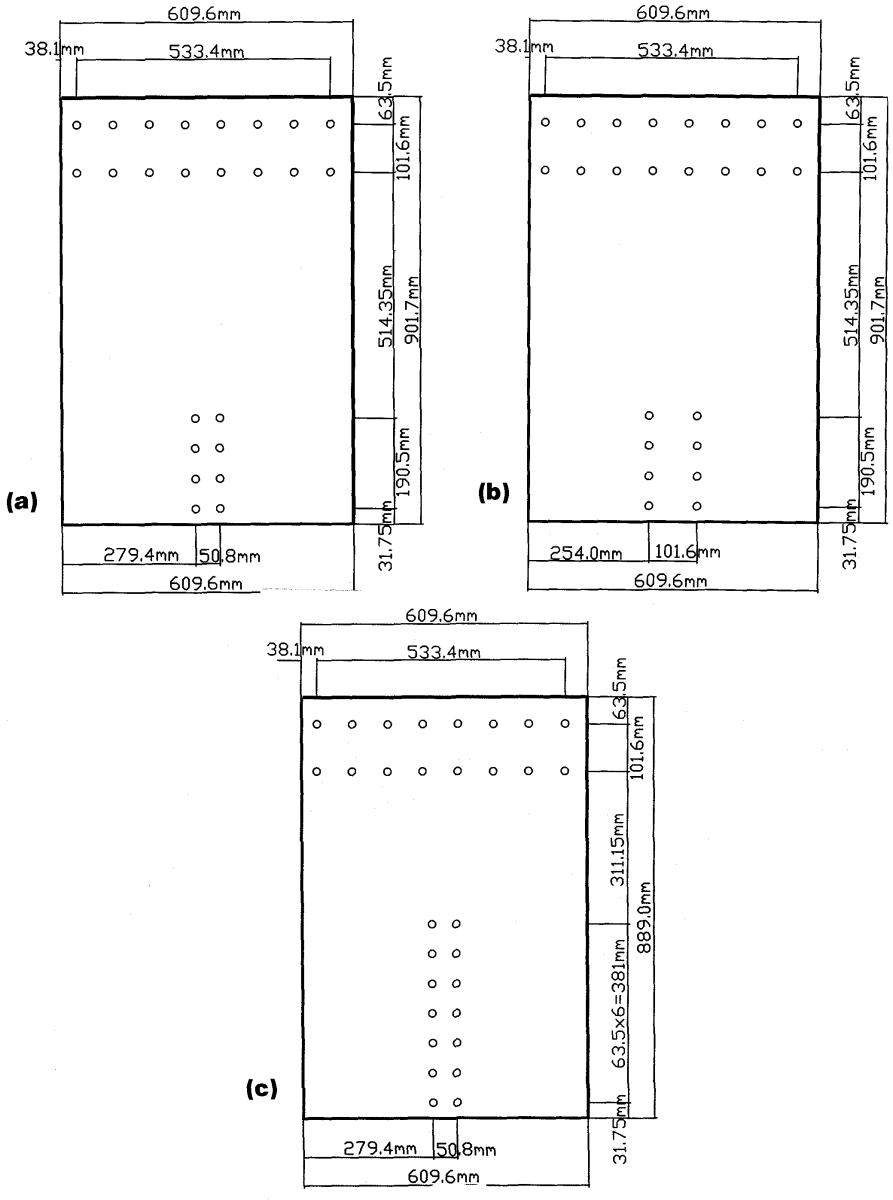

Fig. 2 Schematic showing geometry of the samples: (a) sample SH1, (b) sample SH2, and (c) sample SH3

Upon removal of the initial load train tolerance and a transition into bearing, the test record showed a linear load-displacement region followed by strain hardening into the plastic region. At and beyond the ultimate capacity of the gusset plate the specimens exhibited a progressive decrease in load-carrying capability culminating in failure of the ligaments in tension. The load-carrying capability continued to drop until the termination of testing. The load-deformation response for each specimen type is exemplified in Fig. 4. Test results are summarized in Table 2. None of the curves revealed a well-defined yield point, typical of the family of nonferrous alloys. Rather, the occurrence of yielding was gradual and very similar to the behavior of a coupon in a uniaxial tensile test.

Failure of the ligaments occurred as a direct result of tensile stresses between the upper-row fasteners (bolts). The occurrence of failure by shear was not evident. The ambient temperature tensile properties of alloy 5083-H321 are summarized in Table 3. Also included are the guaranteed minimum and typical as-received mechanical properties. The experimental results suggest that the 5083-H321 plate used in this study can be considered representative of standard mill practice.

3.2 Failure-Damage Analysis

Samples were prepared from the deformed and failed sample (SH2) and examined in a JEOL (JEOL Ltd., Medford, MA) SEM. Sections from the tensile overload region of the sample (SH2) were also removed for examination. Representative fractographs are shown in Fig. 5. An attempt is made to correlate the intrinsic fracture surface features with load (stress) transfer within the bolt group of the connection plate.

High magnification observations of the fracture surface revealed a bimodal failure comprising:

- A large population of voids of varying size and shape and isolated pockets of shallow dimples—features reminiscent of locally ductile mechanisms.
- Numerous fine microscopic cracks and randomly distributed cracked second-phase particles—features reminiscent of locally brittle mechanisms.

The macroscopic voids initially form because of failure of the second-phase particles by cracking. Coalescence of the macroscopic voids occurred by the formation of void sheets and was exacerbated by the intense strain localization between the expanding or growing voids. The highly localized deformation is associated with the formation of microscopic voids at the intermediate-size second-phase particles upon reaching a critical value of local strain. The transgranular fracture regions revealed a highly deformed matrix reminiscent of localized plastic deformation, referred to henceforth as microplasticity of the deforming matrix.

The presence of voids transforms the polycrystalline aluminum alloy into a composite with two populations of particles: grains and voids (a void being considered as a particle having zero stiffness). Because the voids are intrinsically softer than the hardened grains in the aluminum matrix, the local strain is exacerbated for the voids, causing a gradual increase in the volume fraction of voids. The presence of a population of voids of varying size and shape transforms the macroscopic mechanical response of the polycrystalline aluminum alloy. While the macroscopic failure mode was normal to the far-field stress axis and essentially brittle, the microscopic features revealed the occurrence of locally brittle and ductile mechanisms.

Table 2 Summary of mechanical test results

Specimen No.	Maximum load, $N \times 10^3$
SH1	402
SH2	529
SH3	725

Table 3 Room temperature tensile properties of aluminum alloy 5083

Sample	Typical yield strength, σ_{ys}, MPa	Typical ultimate strength, σ_{UTS}, MPa	Design yield strength, σ_{ys}, MPa	Design ultimate strength, σ_{UTS}, MPa	Test yield strength, σ_{YS}, MPa	Test ult. strength, σ_{UTS}, MPa
SH1	228	317	214	303	234	317
SH2	228	317	214	303	245	314
SH3	228	317	214	303	246	329

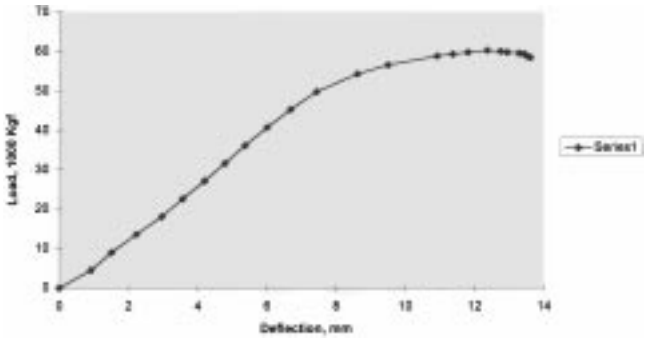

Fig. 3 Typical load-displacement behavior of a connection plate

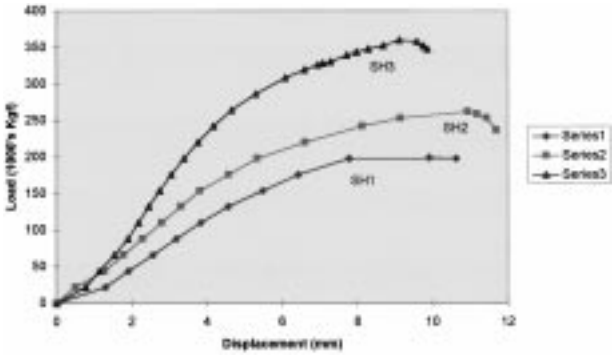

Fig. 4 Comparison of the load versus displacement response for the specimens SH1, SH2, and SH3

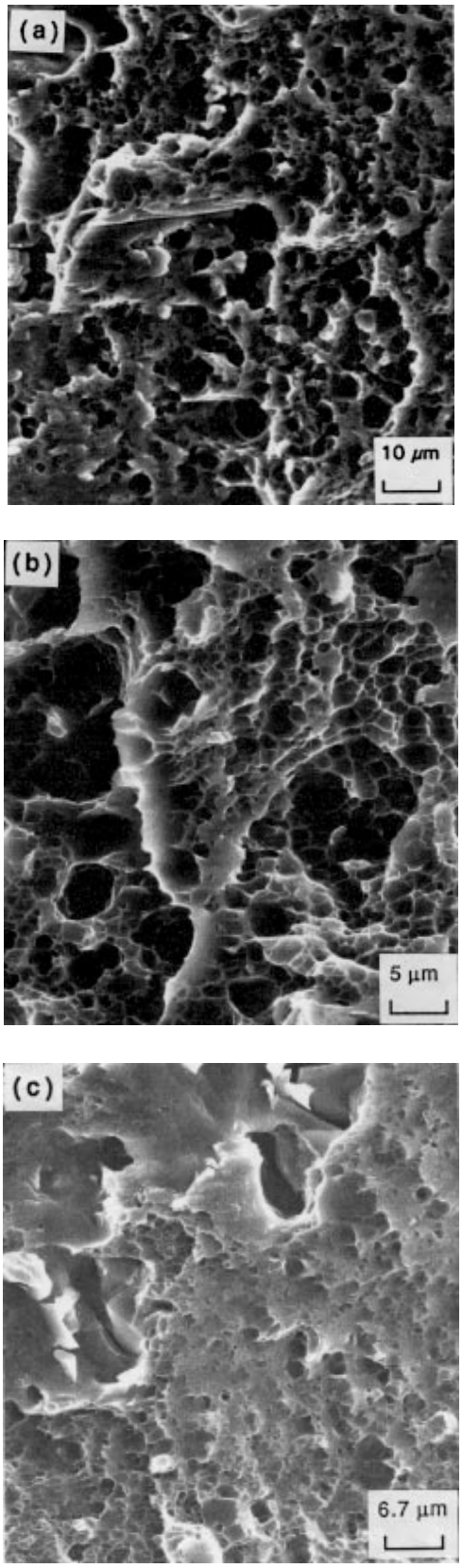

Fig. 5 Scanning electron micrographs of the failed surface of sample SH2 showing (a) a region of tensile overload, (b) microvoid coalescence, and (c) evidence of localized microplastic deformation

3.3 Stress Analysis

Detailed stress analysis was conducted on sample type SH1 using the finite element (FE) method. Two-dimensional, eight-node solid elements were utilized for the mesh of the gusset plate. The FE model comprised a total of 1,572 elements and 4,841 nodes. The element type was chosen to conform with the tolerance of irregular elements required for the areas immediately adjacent to the boundaries of the bolt holes and for automatic mesh generation. The element possesses plasticity and large strain and deformation capabilities. The plate in entirety was modeled, and no attempt was made to incorporate the bolt, fixture, or test machine compliance. The loads were applied as a pressure to the top edge of the mesh. Boundary conditions were simulated by constraining nodes both at and around the bottom half of the holes. A piecewise linear approximation of the stress-strain curve for aluminum alloy 5083-H321 was used in the model. The uniaxial stress-strain behavior was devel-

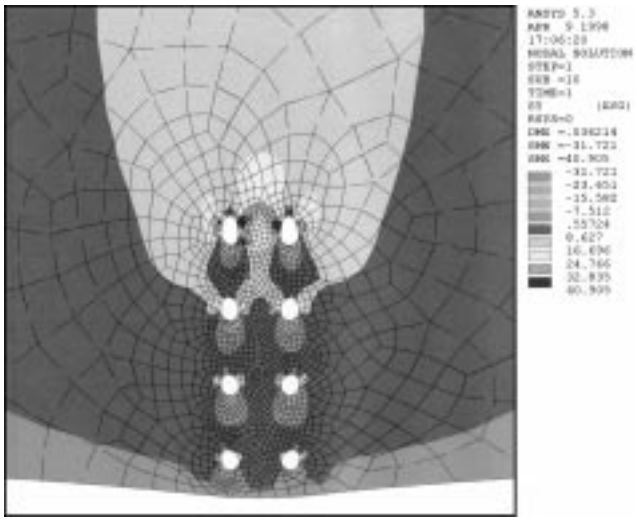

Fig. 6 Normal stress contours for specimen type SH1 under a 22,686 kg loading

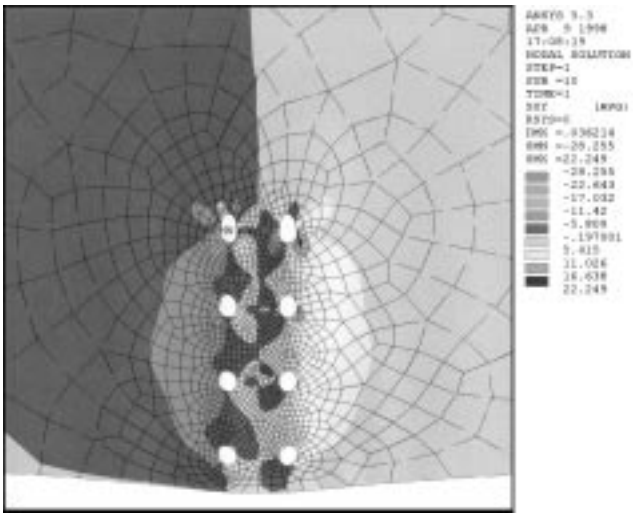

Fig. 7 Shear stress contours for specimen type SH1 under a 22,686 kg loading

oped from standard coupon tests. Analyses were conducted for loads of 22,700 kgf and 40,800 kgf.

A contour plot of the primary (vertical or normal) stress component for the connection plate under the influence of a 22,700 kgf load is shown in Fig. 6. The loading would be expected to result in essentially elastic behavior at the global level. However, some localized regions exist around the sides of the uppermost bolt holes where stress levels are above the monotonic yield strength of alloy 5083-H321 resulting in the occurrence of localized microplastic deformation. The sides of the holes represent points of maximum localized stress concentration. Figure 7 shows the in-plane shear-stress distribution for the area immediately adjacent to the bolt holes under the influence of a 22,700 kgf external load. The shear stress appears to be essentially uniform outside the periphery of the connection and adjacent to the line of bolt holes. The occurrence of localized yielding in shear would be expected to occur when the stress reaches approximately 126 MPa.

Figures 8 and 9 are contour plots of the normal and in-plane shear stress components for the connection plate under an external load of 40,800 kgf. This load is close to the value at which failure of sample (SHl) occurred during mechanical testing. Between the uppermost bolt holes, the normal (i.e., vertical) stress (Fig. 8) reached a level above the ultimate tensile stress for aluminum alloy 5083-H321. The pattern is indicative of localized redistribution of stresses promoting the rapid initiation of both microscopic and macroscopic voids and exacerbated by tensile tearing at regions close to the holes. Other holes in the immediate vicinity showed an increase in the normal stress component, below the level of the uppermost row of holes. The accompanying in-plane shear stress distribution is shown in Fig. 9. Again, the shear stress outside the periphery of the connection appears uniform and approximately equal to the shear yield stress of the material (126 MPa).

3.4 Development of the Failure Model

Several different free-body diagrams can be chosen that essentially isolate the connection area of a generic gusset plate (Fig. 10). The primary load transfer mechanism remains ten-

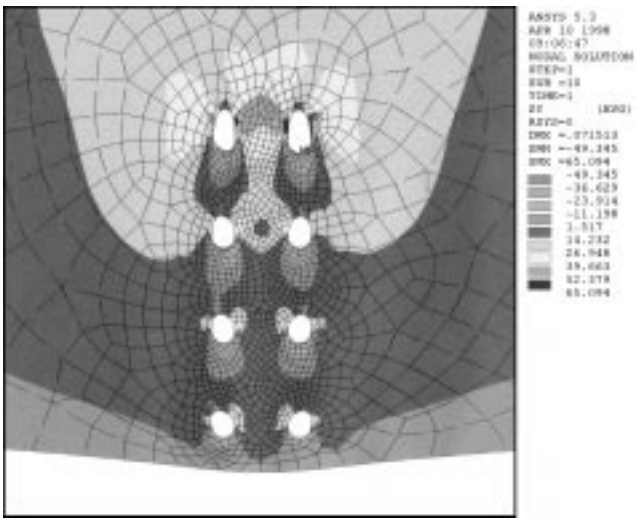

Fig. 8 Normal stress contours for specimen type SH1 under a 40,835 kg loading

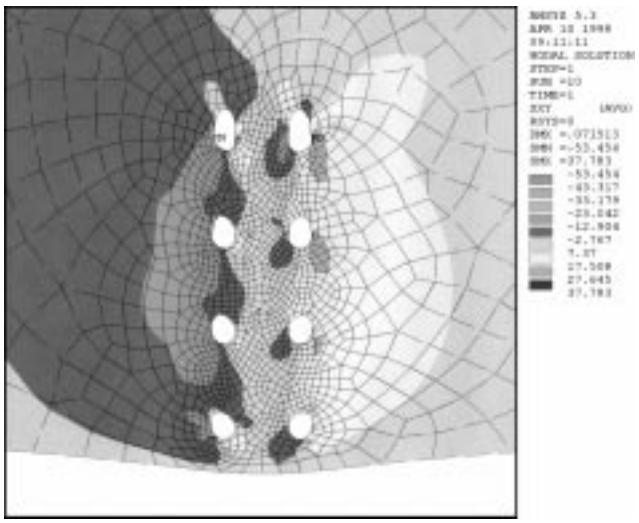

Fig. 9 Shear stress contours for specimen type SH1 under a 40,835 kg loading

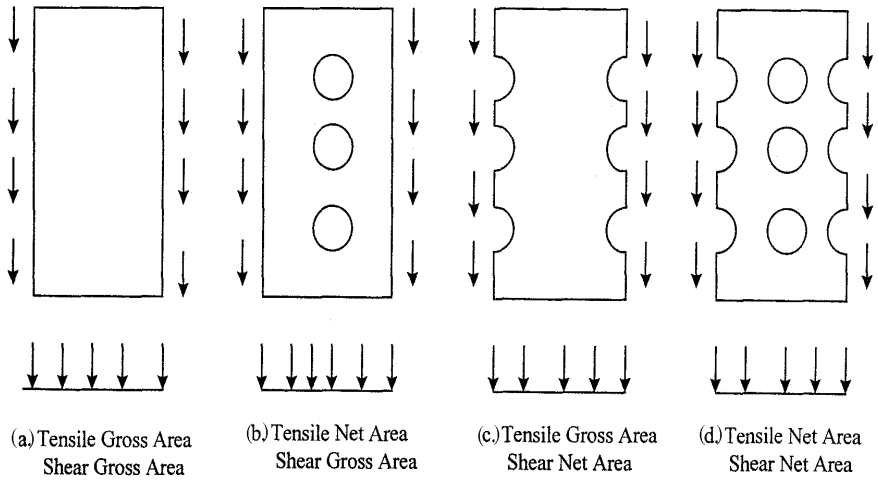

Fig. 10 Schematic of the free-body diagrams of bolt group area

sion at and along the upper row of fasteners and shear along the length of the bolt lines. However, differences exist as to the specific areas over which the tensile and shear forces act. The four possible combinations are:

- *Model combination No. 1:* Conjoint influence of tension and shear acting on the gross area [$P = A_{gt} \cdot \sigma_u + A_{gv} \cdot 0.6\sigma_y$]
- *Model combination No. 2:* Tension acting on the net area with shear acting on the gross area [$P = A_{nt} \cdot \sigma_u + A_{gv} \cdot 0.6\sigma_y$]
- *Model combination No. 3:* Tension acting on the gross area while shear acts on the net area [$P = A_{gt} \cdot \sigma_u + A_{nv} \cdot 0.6\sigma_y$]
- *Model combination No. 4:* Both tension and shear acting along the net areas [$P = A_{nt} \cdot \sigma_u + A_{nv} \cdot 0.6\sigma_y$]

where P is the predicted failure load of the connection plate, A_{gt} is the gross tensile area, A_{nt} is the net tension area, A_{gv} is the gross shear area, A_{nv} is the net shear area, σ_u is the ultimate tensile strength, and σ_y is the yield strength of the aluminum alloy 5083.

Yielding in monolithic alloys of aluminum is relatively insensitive to the hydrostatic stress components and is more influenced by the deviator stress (Ref 11, 12). This forms the basis for the von Mises yield criterion. Yielding in pure shear occurs when the local stress reaches 0.6 times the tensile yield stress.

An evaluation of the four different free-body diagrams and resultant models is based upon previously developed and accepted methodology (Ref 13, 14). A professional factor, defined as the ratio of the ultimate load determined during tests of individual samples to the calculated model connection strength, is evaluated. This can be represented mathematically as professional factor = ultimate test load / model prediction.

An agreement between experimental and analytical results is indicated by a factor either close to or equal to 1.0. Aluminum alloy structures are typically designed on the basis of guaranteed minimum mechanical properties. However, actual properties are often in excess of the guaranteed minimum values. Hence, the model should be judged not only on the basis of measured properties, but whether conservative estimates of connection strength result when calculated from guaranteed minimum tensile properties. A conservative result is interpreted as a professional factor greater than 1.0.

A complete descriptive model would include the effects of connection length. In a bolted joint loaded in shear, the efficiency of the joint would be expected to decrease as the connection length increases. While the overall failure load may increase, it would do so at a decreasing rate. Such behavior can be best described in terms of an average shear stress. As the joint length is increased, the fasteners toward the center of the connection carry a smaller portion of the applied load. The presence of more fasteners in the longer joints will cause the average shear stress to decrease. In light of the four models examined, connection length would be expected to affect the contribution from shear. For short joints the average stress approaches the ultimate strength in shear. However, for very long connections the average stress drops below the expected yield stress in shear. An approach to incorporate length into the model would be to include the use of an effective stress on the shear area. The effective stress would vary between the ultimate strength and yield strength in shear. An effective stress is defined as:

$$\sigma_{eff} = 0.6 \cdot \sigma_y + 0.6 \cdot Cl \cdot (\sigma_u - \sigma_y)$$

where σ_{eff} is the effective stress in shear, σ_y is the yield strength of alloy 5083-H321, σ_u is the ultimate strength of alloy 5083-H321, and Cl is the connection length factor.

Four block shear models have been compared to test results of aluminum connection plates fabricated from alloy 5083-H321. Data analyses indicate that model 2, which utilizes rupture on the net tensile area and yielding on the gross shear area, provides a realistic estimate of connection strength when measured mechanical properties are utilized. For the designer, model 1 results in conservative estimates of block shear behavior when guaranteed minimum properties are employed. The variation of professional factor, calculated using model combination No. 2, for the three different sample types (21 representing sample SHl, 22 representing sample SH2, and 23 representing sample SH3), as a function of uniaxial tensile property (design, experimental and typical) of the aluminum alloy is shown in Fig. 11.

Examination of typical fracture surface features revealed damage mechanisms consistent with model assumptions. Dimple rupture and microvoid coalescence were observed in the tensile overload region of sample SH2. Elongated dimples and voids were found along the fastener lines (what would be considered the area in shear). Other features associated with the failures were observed as well, including development of linear cracking, failure of particles and development of microplasticity.

5. Conclusions

Based on an experimental and numerical study of the mechanical response and failure characteristics of connecting elements in aluminum alloy 5083-H321, key observations are:

- Block failure is a potential limit state for connection plates with mechanical fasteners and should be considered in the design of safe and reliable connections.

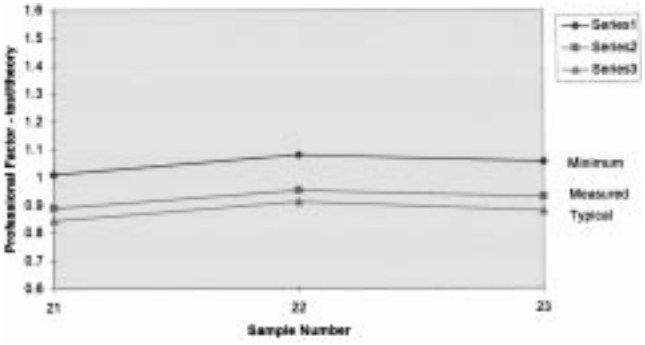

Fig. 11 Variation of professional factor calculated using model combination No. 1, as a function of the (minimum) design, experimental, and typical tensile properties. SH1 = 21, SH2 = 22, and SH3 = 23

- The average failure stress is dependent on length of the connection. Total capacity or strength of the joint increases with an increase in length of the connection.
- Tensile stresses between the uppermost row of fasteners reach a level resulting in failure of the ligaments between fastener holes.
- A design model given by: $P = A_{nt} \cdot \sigma_u + 0.6 \cdot A_{gv} \cdot \sigma_y$ provides a realistic estimate of joint strength when using measured tensile properties. Application of guaranteed minimum values results in conservative estimates of the ultimate strength.
- Damage accumulation mechanisms observed on failure surfaces are consistent with the assumptions used in development of the predictive model.
- Results of finite element stress analysis accord well with choice of model combination No. 2 for overall failure of the connection plate.

References

1. "AAASHTO I LRFD Bridge Design Specifications, Section 7-Aluminum Structures," American Association of State Highway and Transportation Officials, Washington, D.C., 1994
2. The Aluminum Design Manual, The Aluminum Association, Washington, D.C., 1994
3. J.W. Fisher and J.H. Struik, *A Guide to Design Criteria for Bolted and Riveted Joints*, John Wiley & Sons, Inc., 1974
4. M.L. Sharp, *Behavior and Design of Aluminum Structures*, McGraw-Hill, 1993
5. P.C. Birkemoe and M.J. Gilmor, Behavior of Bearing Critical Double-Angle Beam Connections, *AISC Engineering Journal*, American Institute of Steel Construction, 4th Quarter, 1978
6. C. Marsh, Tear-Out Failure of Bolt Groups, American Society of Civil Engineers, *ASCE Structural Journal*, No. ST10, October, 1979
7. R.E. Sanders, Jr., S.F. Baumann, and H.C. Stumpf, *Aluminum Alloys Contemporary Research and Applications: Treatise in Materials Science and Technology*, Vol 31, A.K. Vasudevan and R.D. Doherty, Ed., Academic Press, 1989, p 65-90
8. D. Altenpohl, *Aluminium Viewed from Within*, Aluminium-Verlag GmbH, 1982
9. C. Menzemer and L. Fei, "Design Criteria for Bolted Connection Elements in Aluminum Alloys," Final Technical Report, The Aluminum Association, Washington, D.C., Feb 1998
10. "Measurements Group, System 5000 Model 5100 Scanner-Instruction Manual," Measurements Group, Inc., Instruments Division, Raleigh, NC, 1995
11. R.W. Hertzberg, *Deformation and Fracture Mechanics of Engineering Materials*, 2nd ed., John Wiley & Sons, 1983
12. W.F. Chen and D.J. Han, *Plasticity for Structural Engineers*, Springer-Verlag, 1988
13. S. Haradash and R. Bjorhoude, New Design Criteria for Gusset Plates in Tension, *AISC Engineering Journal*, American Institute for Steel Construction, 2nd Quarter, 1985
14. T.V. Galambos, Load and Resistance Factor Design, *AISC Engineering Journal*, American Institute for Steel Construction, 3rd Quarter, 1981
15. *Aluminum Standards and Data*, The Aluminum Association, Washington, D.C., 1988